Journal of Neurology (2019) 266:1887–1896
https://doi.org/10.1007/s00415-019-09350-9

ORIGINAL COMMUNICATION

# Cortical microinfarcts in patients with multiple lobar microbleeds on 3 T MRI

Yuichiro Ii[1] · Masayuki Maeda[2] · Hidehiro Ishikawa[1] · Ai Ito[1] · Ko Matsuo[1] · Maki Umino[3] · Akihiro Shindo[1] · Hirotaka Kida[4] · Masayuki Satoh[4] · Atsushi Niwa[1] · Akira Taniguchi[1] · Hidekazu Tomimoto[1]

Received: 14 January 2019 / Revised: 13 April 2019 / Accepted: 26 April 2019 / Published online: 2 May 2019


## Abstract

The pathogenesis of cortical microinfarcts (CMIs) is considered to be heterogeneous including cerebral small vessel disease (SVD) such as hypertensive vasculopathy (HV) and cerebral amyloid angiopathy (CAA). Recent advances in MRI have enabled the detection of CMIs in vivo. To investigate the characteristics of CMIs in advanced cerebral SVD, we performed a retrospective analysis of 85 patients with cognitive impairment who had multiple lobar cerebral microbleeds (CMBs) on 3 T MRI. Among them, 41 (48.2%) patients were classified into the strictly lobar CMB group (i.e. probable-CAA group), and 44 (51.8%) patients were classified into the non-lobar with lobar CMBs group (i.e. mix-CMBs group). The relationship between CMIs and CMBs, cortical superficial siderosis (cSS) and white matter hyperintensity was evaluated. Nine of the 41 (22.0%) patients with probable-CAA had a total of 19 CMIs, while 12 of the 44 (27.3%) patients with mix-CMBs had a total of 38 CMIs. In the probable-CAA group, the presence of CMIs was significantly associated with the presence of cSS ($p < 0.001$). In addition, a close spatial association between CMIs and cSS was observed. On the contrary, in the mix-CMB group, the presence of CMIs was significantly associated with the number of lobar CMBs in the frontal lobe ($p = 0.034$). Our results suggest that CMIs in the probable-CAA may be attributable to more severe CAA, while CMIs in the mix-CMBs indicate an advanced HV, especially when observed with more numerous lobar CMBs.

**Keywords** Cortical microinfarcts · Cerebral microbleeds · Cerebral amyloid angiopathy · Hypertensive vasculopathy · Cortical superficial siderosis · Magnetic resonance imaging

## Introduction

Cortical microinfarcts (CMIs) are frequently detected in the brains of elderly subjects at autopsy as small foci with diameters ranging from 50 μm to a few millimeters. They are restricted to the cerebral cortex, and could be related to cognitive impairment [1]. The pathogenesis of CMIs may be heterogeneous and has been presumed to be caused by cerebral small vessel disease (SVD), microembolism and hypoperfusion [2]. It is believed that small cortical vessel eventually occludes and leads to CMI although the pathogenic mechanism has not been fully elucidated. In the cerebral SVD, CMIs usually occur at the latest stage [3].

Cerebral amyloid angiopathy (CAA) and hypertensive vasculopathy (HV) are two representative forms of cerebral SVD. CAA is associated with multiple strictly lobar cerebral microbleeds (CMBs), cortical superficial siderosis (cSS) and a posterior distribution of white matter hyperintensity (WMH) [4]. Although a pathological examination is the gold standard for the diagnosis of CAA, the condition can be diagnosed noninvasively according to the modified Boston criteria in the setting of lobar intracranial hemorrhage (ICH), lobar CMBs and cSS [5]. A recent study has suggested that the presence of multiple ($\geq 2$) strictly lobar CMBs is a specific finding for moderate to severe CAA even in the absence of lobar ICH [6]. This finding—in addition to the Boston criteria—may strengthen the diagnosis of probable-CAA

✉ Yuichiro Ii
ii-y@clin.medic.mie-u.ac.jp

1 Department of Neurology, Mie University Graduate School of Medicine, 2-174 Edobashi, Tsu, Mie 514-8507, Japan

2 Department of Advanced Diagnostic Imaging, Mie University Graduate School of Medicine, Tsu, Mie, Japan

3 Department of Radiology, Mie University Graduate School of Medicine, Tsu, Mie, Japan

4 Department of Dementia Prevention and Therapeutics, Mie University Graduate School of Medicine, Tsu, Mie, Japan

[7]. In contrast, HV is associated with deep/infratentorial (i.e. non-lobar) CMBs, lacunar infarction and WMH with no predilection for brain region including peri-basal ganglia [8]. Mixed (non-lobar with lobar) CMBs are also thought to reflect HV, but the synergistic effects of HV and CAA may also contribute to the development of mixed CMBs [9, 10].

Until recently, CMIs have remained invisible on conventional MRI. We first reported the in vivo detection of CMIs using 3-Tesla (3 T) MRI with the combination of three-dimensional double inversion recovery (3D-DIR) and three-dimensional fluid attenuated inversion recovery (3D-FLAIR) [11]. The small high-intensity intracortical lesions present on these images were demonstrated to represent pathological CMIs in our radiological–histopathological correlation studies [12, 13]. Several studies on CMIs using 3 T or 7 T MRI have been reported in both hospital and population-cohort settings [14–21]. However, no research has focused on CMIs in patients with multiple lobar CMBs. CMBs are considered to represent focal accumulation of hemosiderin-laden macrophages indicating a small amount of previous bleeding from advanced cerebral SVD [22]. Therefore, multiple lobar CMBs are considered to indicate widespread severe arteriopathy in lobar location, including small penetrating cortical vessels. From this point of view, we focused on CMIs in patients with multiple lobar CMBs which may represent advanced cerebral SVD. We aimed to investigate the relationship between CMIs and other neuroimaging markers of SVD in patients with multiple lobar CMBs (either with strictly lobar or mixed CMBs), and thereby making it clear the characteristics of CMIs between these two groups.

## Methods

### Study subjects and data collection

We performed a retrospective analysis of our database of 215 patients with cognitive impairment (male, $n = 86$; mean age, $75.8 \pm 7.7$ years) who were recruited from the Department of Neurology and Memory Clinic of Mie University Hospital between August 2009 and July 2013. Of these, 127 were diagnosed with Alzheimer's disease (AD), 11 with AD with cerebrovascular disease, 50 with mild cognitive impairment, 16 with vascular dementia, and 11 with other disorders. All diagnoses were based on respective pre-established criteria [23–26]. Their average Mini-Mental State Examination (MMSE) score was $22.2 \pm 4.9$ (mean $\pm$ SD). Patients with single lobar CMBs or strictly deep CMBs were excluded from this analysis. Patients without CMBs were also excluded. Finally, patients with multiple ($\geq 2$) lobar CMBs were included in this analysis. Then, patients with multiple ($\geq 2$) lobar CMBs were classified according to the distribution of their CMBs into strictly lobar (i.e. probable-CAA based on the Boston criteria [5, 7]) and mixed (i.e. mix-CMBs).

The demographic and clinical information was obtained by a review of the patients' medical records. In all patients, the presence of hypertension, hyperlipidemia, and diabetes was determined based on a prior medical diagnosis and treatment. Smoking was defined by a history of tobacco use. We compared the characteristics of the included (those with multiple lobar CMBs) and excluded patients (those without) to assess the selection bias.

This study was approved by the ethical review board of Mie University Hospital and the requirement for written informed consent was waived because of the retrospective study design. This study was performed in accordance with the ethical standards established in the 1964 Declaration of Helsinki and its subsequent amendments.

### Neuroimaging data and analyses

The MRI studies were performed with a 3 T MR unit (Achieva, Philips Medical System, Best, The Netherlands) as described previously [11]. DIR imaging was performed using two different inversion pulses. The long inversion time and short inversion time were defined as the intervals between the 180° inversion pulse and the 90° excitation pulse, respectively, which was optimized for human brain imaging by the vendor. The 3D DIR settings were as follows: field of view, 250 mm; matrix, $208 \times 163$ ($256 \times 256$ after reconstruction; in-plane resolution, 0.98 mm $\times$ 0.98 mm); section thickness, 0.65 mm (contiguous slices); TSE factor 173; repetition time (ms)/echo time (ms), 5500/247; long inversion time (ms)/short inversion time (ms), 2550/450; number of signals acquired, two; and acquisition time, 5 min 13 s for 3D. 3D FLAIR imaging was obtained in a sagittal direction; then, axial and coronal images were reconstructed. The 3D FLAIR settings were as follows: field of view, 260 mm; matrix, $288 \times 288$ ($364 \times 364$ after reconstruction; in-plane resolution, $0.68 \times 0.67$ mm); section thickness, 1 mm with 0.5 mm overlap; no parallel imaging; repetition time (ms)/echo time (ms), 6000/400; inversion time, 2000 ms; number of signals acquired, two; and acquisition time, 5 min 12 s. Regarding 3D FLAIR and 3D DIR, axial and coronal images with a slice thickness of 1 mm were also reconstructed from the 3D data, and were used for the evaluation of CMIs. Intracortical lesions were considered to be positively detected if they were exclusively detected as high signal foci on both 3D DIR and 3D FLAIR. Susceptibility-weighted imaging (SWI) was performed to detect CMBs and cSS. The SWI settings were follows: field of view, 230 mm; matrix, $320 \times 251$ ($512 \times 512$ after reconstruction; in-plane resolution, 0.45 mm $\times$ 0.45 mm); section thickness, 0.5 mm (contiguous slices); minIP with 5 mm, repetition time (ms)/

echo time (ms), 22/11.5 (in-phase), 33 (shifted); number of signals acquired, one; flip angle 20° and acquisition time, 5 min 45 s. To achieve optimal diagnostic quality images, SWI was displayed in the transverse plane with a slice thickness of 1.6 mm.

CMB, WMH and lacunar infarction were defined according to the STandards for ReportIng Vascular changes on nEuroimaging (STRIVE) consensus [27]. The topographical distribution of CMB was evaluated using the Microbleed Anatomical Rating Scale (MARS) [28]. WMH was assessed using the age-related white matter changes (ARWMC) scale [29]. cSS was defined by the presence of linear residues of chronic blood products in the superficial layers of the cerebral cortex showing a characteristic gyriform pattern of a low signal on SWI and was excluded if it was contiguous with any ICH [30]. CMI was defined as an intracortical lesion (≤5 mm) detected as high signal foci on both 3D DIR and 3D FLAIR images [11]. Images were analyzed by one neurologist (Y. I.) and two neuroradiologists (M. U. and M. M.) who were blinded to clinical data. Lesions with complete agreement by all raters were included.

## Statistical analyses

All statistical analyses were performed using the SPSS software program (version 21 for Windows IBM Corp.). We explored the differences in the baseline characteristics of the included and excluded patients. We then assessed the clinical characteristics and MRI findings of patients with and without CMIs in the probable-CAA and mix-CMB groups. The $\chi^2$ test or Fisher's exact test was used for categorical variables and Student's *t* test or the Mann–Whitney test was used for continuous variables. To investigate the odds ratios for the presence of CMI, a multivariable logistic regression analysis was performed with covariates related to the presence of CMI in the univariate analysis. Covariates were inputted using the incremental stepwise method. In addition, we compared the characteristics of CMIs (relationship to MRI markers, count, size, prevalence in each cerebral lobe, spatial relationship to CMBs and cSS) between the probable-CAA and mix-CMB groups using the $\chi^2$ test or Fisher's exact test for categorical variables and Student's *t* test for continuous variables. *p* values of $<0.05$ were considered to indicate statistical significance in all analyses.

## Results

Of the 215 patients, 41 had single lobar or strictly deep CMBs and 89 had no CMBs, so 85 patients with multiple (≥2) lobar CMBs were included in the final analysis. Those who were excluded were not significantly different from those included in the analysis except for the average MMSE score and the prevalence of hypertension (Table 1). Among the 85 patients with multiple (≥2) lobar CMBs, 41 (48.2%) patients showed probable-CAA and the remaining 44 (51.8%) patients showed mix-CMBs. The clinical characteristics of the 85 patients are shown in Table 2. CMIs were detected in 9 of the 41 (22.0%) patients in the probable-CAA group, and 12 of the 44 (27.3%) patients in the mix-CMB group ($p=0.57$). A flowchart of the patient selection is shown in Fig. 1. Representative images of CMIs from one patient each in the probable-CAA and mix-CMB groups are shown in Fig. 2.

## Comparison between the probable-CAA patients with or without CMIs

There were no significant differences in age, gender, MMSE score, or the prevalence of vascular risk factors between probable-CAA patients with or without CMIs. The patients with CMIs had significantly more lobar CMBs in the whole cerebral lobe ($p=0.031$), frontal lobe ($p=0.035$) and parietal lobe ($p=0.015$) in comparison with those without CMIs. Furthermore, the WMH in the whole brain, and the frontal and the parieto-occipital lobes was significantly more severe in the patients with CMIs than in those without CMIs (whole brain, $p=0.029$; frontal lobe, $p=0.013$; parieto-occipital lobe, $p=0.024$). The prevalence of lobar ICH and cSS in the patients with CMIs was significantly higher than those in patients without CMIs (lobar ICH, $p=0.031$; cSS, $p<0.001$) (Table 3). A multivariable logistic regression analysis adjusted for age and gender revealed that the presence of CMI was inversely associated with the absence of cSS in the probable-CAA group [OR 0.013; (95% CI 0.001–0.142); $p<0.001$].

**Table 1** Characteristics of the included and excluded patients

| | Included ($n=85$) | Excluded ($n=130$) | *p* value |
|---|---|---|---|
| Age, years, mean ± SD | 75.9 ± 8.8 | 75.7 ± 6.9 | 0.877 |
| Male, *n* (%) | 36 (42.4) | 50 (38.5) | 0.509 |
| MMSE, mean ± SD | 21.1 ± 5.2 | 22.8 ± 4.7 | 0.017* |
| Hypertension, *n* (%) | 49 (57.6) | 46 (35.4) | 0.001* |
| Diabetes mellitus, *n* (%) | 13 (15.3) | 25 (19.2) | 0.459 |
| Dyslipidemia, *n* (%) | 23 (27.1) | 24 (18.5) | 0.136 |
| Smoking, *n* (%) | 13 (15.3) | 13 (10.0) | 0.244 |

MMSE, Mini-Mental State Examination; SD, standard deviation

*$p<0.05$ for included vs. excluded

**Table 2** Characteristics in patients with probable-CAA and mix-CMBs

| | All ($n=85$) | Probable-CAA ($n=41$) | Mix-CMBs ($n=44$) | $p$ value |
|---|---|---|---|---|
| Age, years, mean ± SD | 75.9 ± 8.8 | 75.9 ± 9.9 | 76.6 ± 9.6 | 0.985 |
| Male, *n* (%) | 36 (42.4) | 19 (46.3) | 17 (38.6) | 0.473 |
| MMSE, mean ± SD | 21.1 ± 5.2 | 20.9 ± 5.9 | 21.3 ± 4.6 | 0.751 |
| Hypertension, *n* (%) | 49 (57.6) | 16 (39.0) | 33 (75.0) | 0.001* |
| Diabetes mellitus, *n* (%) | 13 (15.3) | 6 (14.6) | 7 (15.9) | 0.870 |
| Dyslipidemia, *n* (%) | 23 (27.1) | 9 (22.0) | 14 (31.8) | 0.306 |
| Smoking, *n* (%) | 13 (15.3) | 7 (17.1) | 6 (13.6) | 0.660 |
| CMI, *n* (%) | 21 (24.7) | 9 (22.0) | 12 (27.3) | 0.570 |
| CMB count, median (IQR) | | | | |
| Lobar | 9 (3–40) | 4 (2–29.5) | 15.5 (4.25–63) | 0.005* |
| Frontal | 2 (1–6) | 1 (1–4) | 3 (1–8) | 0.042* |
| Parietal | 2 (0–13.5) | 1 (0–8.5) | 3 (1–15.75) | 0.172 |
| Temporal | 2 (0–13.5) | 1 (0–6.5) | 7 (1–22.25) | < 0.001* |
| Occipital | 1 (0–3) | 1 (0–2.5) | 1 (0–4.75) | 0.152 |
| Insula | 0 (0–0) | 0 (0–0) | 0 (0–0) | 0.959 |
| Deep | 0 (0–3) | 0 (0–0) | 2.5 (1–7.5) | |
| Infratentorial | 0 (0–1) | 0 (0–0) | 1 (0–4) | |
| WMH, ARWMC, median (IQR) | | | | |
| Whole | 12 (8–17) | 10 (6–14.5) | 16 (10–19) | 0.002* |
| Frontal | 5 (4–6) | 4 (3–6) | 5.5 (4–6) | 0.224 |
| Parieto-occipital | 5 (4–6) | 4 (3–6) | 5.5 (4–6) | 0.044* |
| Temporal | 0 (0–2.5) | 0 (0–2) | 1 (0–3) | 0.071 |
| Infratentorial | 0 (0–0) | 0 (0–0) | 0 (0–6) | 0.019* |
| Basal ganglia | 1 (0–4) | 0 (0–2) | 2 (0–6) | 0.002* |
| Lobar ICH, *n* (%) | 10 (11.8) | 7 (17.1) | 3 (6.8) | 0.186 |
| Lacunes, *n* (%) | 43 (50.6) | 11 (26.8) | 32 (72.7) | < 0.001* |
| cSS, *n* (%) | 14 (16.5) | 11 (26.8) | 3 (6.8) | 0.013* |

ARWMC, age-related white matter changes; CAA, cerebral amyloid angiopathy; CMB, cerebral microbleed; CMI, cortical microinfarct; cSS, cortical superficial siderosis; ICH, intracranial hemorrhage; IQR, interquartile range; mix-CMBs, mixed cerebral microbleeds; MMSE, Mini-Mental State Examination; SD, standard deviation; WMH, white matter hyperintensity

*$p < 0.05$ for probable-CAA vs. mix-CMBs

## Comparison between mix-CMB patients with or without CMIs

There were no significant differences in age, gender, MMSE score, prevalence of vascular risk factors, WMH, lobar ICH, lacunar infarction or cSS between the mix-CMB patients with or without CMIs. The numbers of lobar and infratentorial CMBs were significantly higher in the patients with CMIs than in those without CMIs (lobar CMBs, $p=0.007$; infratentorial CMBs, $p=0.010$), while the number of deep CMBs did not differ to a statistically significant extent (Table 4). In a multivariable logistic regression analysis adjusted for age and gender, the number of lobar CMBs in the frontal lobe was significantly associated with the presence of CMIs in the patients with mix-CMBs [OR 1.058; (95% CI 1.004–1.115); $p=0.034$].

## Characteristics of CMIs in the probable-CAA and mix-CMB patients

On comparing the clinical characteristics and neuroimaging markers between probable-CAA patients with CMIs and mix-CMB patients with CMIs, the prevalence of cSS in the probable-CAA group was significantly higher than in the mix-CMB group (88.9% vs. 8.3%, $p<0.001$). In contrast, the prevalence of hypertension and lacunar infarction in the mix-CMB group was significantly higher than in the probable-CAA group (hypertension 33.3% vs. 91.7%, $p=0.016$; lacunar infarction 33.3% vs. 83.3%, $p=0.032$). Furthermore, the number of CMBs in the temporal lobe and severity of WMH in the whole brain and basal ganglia were significantly higher in the mix-CMB group than in the probable-CAA group (CMBs in the temporal lobe, $p=0.028$; WMH

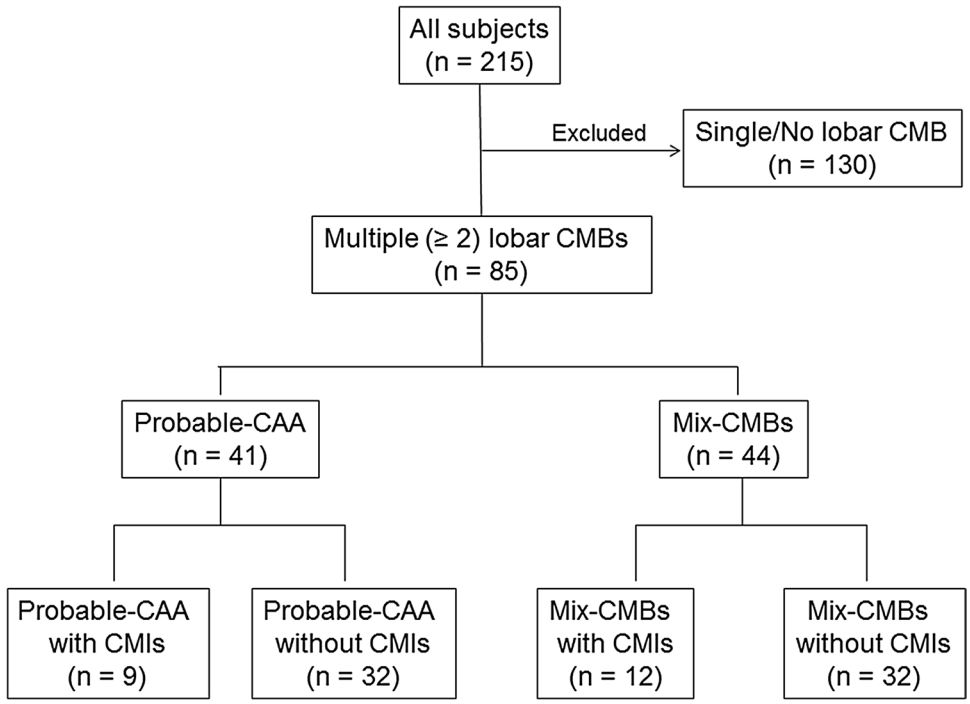


**Fig. 1** Flowchart of patient selection. CMB, cerebral microbleed; CMI, cortical microinfarct; mix-CMBs, mixed cerebral microbleeds; probable-CAA, probable cerebral amyloid angiopathy; SL-CMBs, strictly lobar cerebral microbleeds

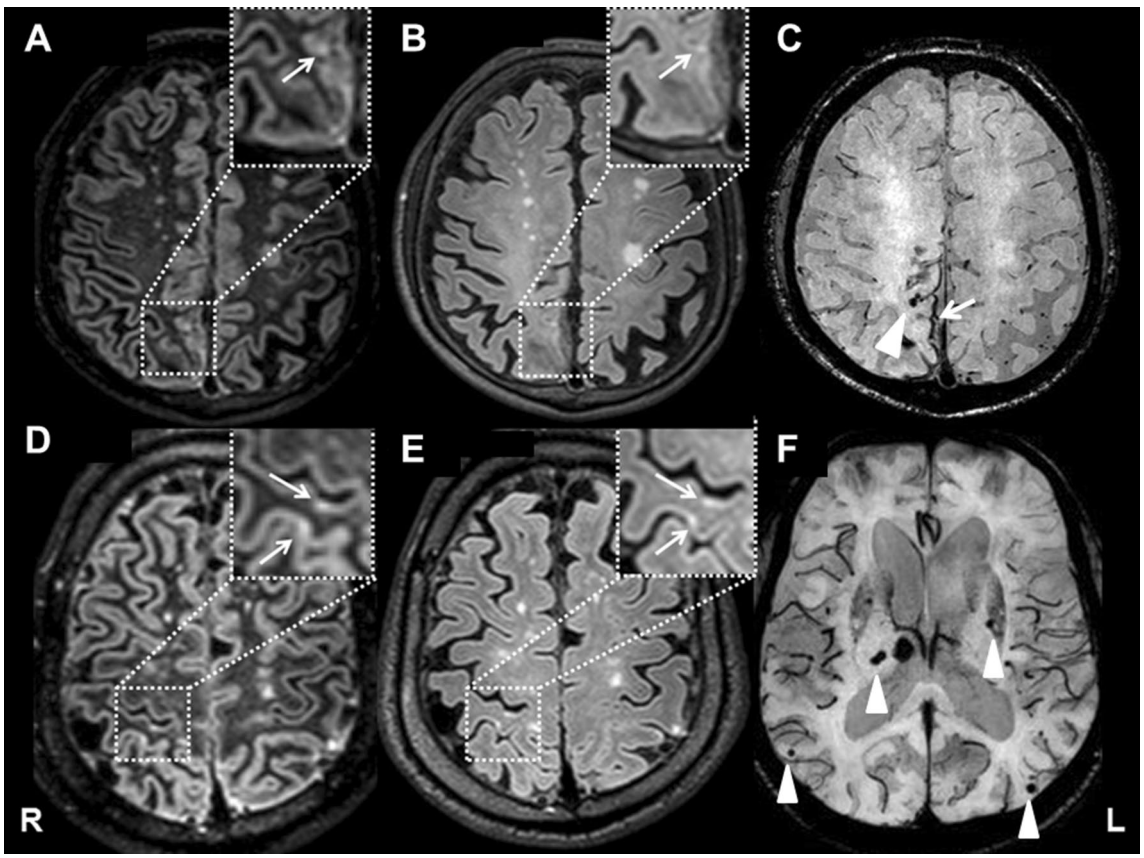


**Fig. 2** Representative images of "Probable-CAA with CMIs" and "Mix-CMBs with CMIs". Image from a patient with probable-CAA with CMIs: 3D DIR (**a**) and 3D FLAIR (**b**) images show cortical microinfarct (CMI) in the right parietal lobe (insert, white arrow). Susceptibility-weighted imaging (SWI) (**c**) shows cortical superficial siderosis (cSS; white arrow) and lobar cerebral microbleeds (CMBs; white arrowhead) in the right parietal lobe. Image from a patient with mix-CMBs with CMIs: 3D DIR (**d**) and 3D FLAIR (**e**) images show CMIs in the right parietal lobe (insert, white arrows). SWI (**f**) shows both deep and lobar CMBs (white arrowheads)

**Table 3** Comparison between probable-CAA patients with or without CMIs

| Patients with probable-CAA | With CMIs ($n=9$) | Without CMIs ($n=32$) | $p$ value |
|---|---|---|---|
| Age, years, mean ± SD | 79.8 ± 4.4 | 74.8 ± 10.8 | 0.184 |
| Male, *n* (%) | 4 (44.4) | 15 (46.9) | 1.000 |
| MMSE, mean ± SD | 22.6 ± 5.3 | 20.5 ± 6.0 | 0.415 |
| Hypertension, *n* (%) | 3 (33.3) | 13 (40.6) | 1.000 |
| Diabetes mellitus, *n* (%) | 2 (22.2) | 4 (12.5) | 0.597 |
| Dyslipidemia, *n* (%) | 1 (11.1) | 8 (25.0) | 0.654 |
| Smoking, *n* (%) | 0 (0.0) | 7 (21.9) | 0.315 |
| CMB count, median (IQR) | | | |
| Lobar | 37 (5–48.5) | 3.5 (2–8.5) | 0.013* |
| Frontal | 4 (1.5–10) | 1 (0.25–3) | 0.035* |
| Parietal | 10 (2.5–17.5) | 1 (0–3.5) | 0.015* |
| Temporal | 8 (5–12.5) | 1 (0–2) | 0.128 |
| Occipital | 2 (0.5–8) | 0 (0–2) | 0.052 |
| Insula | 0 (0–0) | 0 (0–0) | 0.865 |
| WMH, ARWMC, median (IQR) | | | |
| Whole | 14 (11.5–15) | 8 (6–13) | 0.029* |
| Frontal | 6 (5–6) | 4 (3–6) | 0.013* |
| Parieto-occipital | 6 (4–6) | 4 (2–6) | 0.024* |
| Temporal | 0 (0–3) | 0 (0–1.75) | 0.466 |
| Infratentorial | 0 (0–0) | 0 (0–0) | 0.793 |
| Basal ganglia | 0 (0–2.5) | 0 (0–2) | 0.963 |
| Lobar ICH, *n* (%) | 4 (44.4) | 3 (9.4) | 0.031* |
| Lacunes, *n* (%) | 3 (33.3) | 8 (25.0) | 0.680 |
| cSS, *n* (%) | 8 (88.9) | 3 (9.4) | < 0.001* |

ARWMC, age-related white matter changes; CAA, cerebral amyloid angiopathy; CMB, cerebral microbleed; CMI, cortical microinfarct; cSS, cortical superficial siderosis; ICH, intracranial hemorrhage; IQR, interquartile range; MMSE, Mini-Mental State Examination; SD, standard deviation; WMH, white matter hyperintensity

*$p < 0.05$

in the whole brain, $p=0.028$; WMH in the basal ganglia, $p=0.023$).

In the probable-CAA group, 19 CMIs were detected overall: most were found in the parietal lobe ($n=8$; 42.1%) followed by the temporal lobe ($n=4$; 21.1%). In contrast, 38 CMIs were detected overall in the mix-CMB group: most were found in the temporal lobe ($n=14$; 36.8%) followed by the parietal lobe ($n=8$; 21.1%). However, there were no significant differences in the mean number, size or distribution of CMIs between the probable-CAA and mix-CMB groups (Table 5). Although the frequency of CMIs close to CMBs in the same gyrus did not differ to a statistically significant extent between these two groups, the prevalence of CMIs co-existing with cSS in the same cerebral lobe in the probable-CAA group was significantly higher in comparison with the mix-CMB group (21.2% vs. 2.6%, $p=0.038$).

## Discussion

The major findings of our study were as follows. In the probable-CAA group, the presence of CMIs showed a close relationship with cSS. On the other hand, numerous lobar CMBs, especially in the frontal lobe, were related to the presence of CMIs in the mix-CMB group. The characteristics of CMIs in these two groups were not markedly different, except for the probable-CAA group showing a higher prevalence of co-existing with cSS in the same cerebral lobe.

Several histopathological studies have demonstrated a significant association between severe CAA and CMIs [31–34]. In addition, a recent study showed a strong association between CMIs at autopsy and higher numbers of lobar CMBs on antemortem MRI in patients with CAA; thus, it has been suggested that these two types of lesions share

**Table 4** Comparison between mix-CMBs patients with or without CMIs

| Patients with mix-CMBs | With CMIs ($n=12$) | Without CMIs ($n=32$) | $p$ value |
|---|---|---|---|
| Age, years, mean ± SD | 74.2 ± 11.8 | 76.5 ± 5.8 | 0.390 |
| Male, *n* (%) | 5 (41.7) | 12 (37.5) | 1.000 |
| MMSE, mean ± SD | 20.3 ± 4.2 | 21.7 ± 4.7 | 0.388 |
| Hypertension, *n* (%) | 11 (91.7) | 22 (68.8) | 0.240 |
| Diabetes mellitus, *n* (%) | 0 (0.0) | 7 (21.9) | 0.163 |
| Dyslipidemia, *n* (%) | 6 (50.0) | 8 (25.0) | 0.152 |
| Smoking, *n* (%) | 2 (16.7) | 4 (12.5) | 0.658 |
| CMB count, median (IQR) | | | |
| Lobar | 56 (13–235.75) | 12 (4–31.25) | 0.007* |
| Frontal | 7 (3–83.5) | 2.5 (1–4) | 0.009* |
| Parietal | 15.5 (3–54) | 2 (0–9.5) | 0.014* |
| Temporal | 19 (6.25–73.75) | 2 (1–13) | 0.005* |
| Occipital | 6 (2–15.75) | 1 (0–2) | 0.003* |
| Insula | 0 (0–1.75) | 0 (0–0) | 0.055 |
| Deep | 4.5 (1.25–10) | 2 (1–5.75) | 0.255 |
| Infratentorial | 5 (1–12.25) | 1 (0–2) | 0.010* |
| WMH, ARWMC, median (IQR) | | | |
| Whole | 18 (13.75–22.75) | 13.5 (10–18) | 0.112 |
| Frontal | 6 (4–6) | 5 (4–6) | 0.507 |
| Parieto-occipital | 6 (4.5–6) | 5 (4–6) | 0.145 |
| Temporal | 1.5 (0–3) | 0.5 (0–3) | 0.668 |
| Infratentorial | 0 (0–2.75) | 0 (0–0) | 0.161 |
| Basal ganglia | 4 (0.5–6) | 2 (0–6) | 0.341 |
| Lobar ICH, *n* (%) | 1 (8.3) | 2 (6.3) | 1.000 |
| Lacunes, *n* (%) | 10 (83.3) | 22 (68.8) | 0.461 |
| cSS, *n* (%) | 1 (8.3) | 2 (6.3) | 1.000 |

ARWMC, age-related white matter changes; CMB, cerebral microbleed; CMI, cortical microinfarct; cSS, cortical superficial siderosis; ICH, intracranial hemorrhage; IQR, interquartile range; mix-CMBs, mixed cerebral microbleeds; MMSE, Mini-Mental State Examination; SD, standard deviation; WMH, white matter hyperintensity

*$p<0.05$

**Table 5** Characteristics of CMIs in the patients with probable-CAA and mix-CMBs

| | Probable-CAA ($n=9$) | Mix-CMBs ($n=12$) | $p$ Value |
|---|---|---|---|
| CMI count, total | 19 | 38 | |
| Count, mean ± SD | 2.1 ± 1.3 | 3.2 ± 2.6 | 0.281 |
| Size (mm), mean ± SD | 2.8 ± 0.5 | 2.8 ± 0.6 | 0.749 |
| CMI prevalence in each region, *n* (%) | | | |
| Frontal | 3 (15.8) | 7 (18.4) | 1.000 |
| Parietal | 8 (42.1) | 8 (21.1) | 0.095 |
| Temporal | 4 (21.1) | 14 (36.8) | 0.227 |
| Occipital | 3 (15.8) | 5 (13.2) | 1.000 |
| Insula | 1 (5.3) | 4 (10.5) | 0.655 |
| CMI close to CMBs in the same gyrus, *n* (%) | 8 (42.1) | 12 (31.6) | 0.432 |
| CMI in the same cerebral lobe with cSS, *n* (%) | 4 (21.1) | 1 (2.6) | 0.038* |

CAA, cerebral amyloid angiopathy; CMB, cerebral microbleed; CMI, cortical microinfarct; cSS, cortical superficial siderosis; mix-CMBs, mixed cerebral microbleeds; SD, standard deviation

*$p<0.05$

an underlying mechanism [35]. Another histopathological study showed that the MRI-defined CMBs in CAA patients were heterogeneous and partly corresponded to hemorrhagic CMIs [36]. In our study, the probable-CAA patients who had CMIs had a greater number of lobar CMBs than those without CMIs. Furthermore, 42% of CMIs were present in the same cerebral gyrus as lobar CMBs; thus, it seemed reasonable to infer that there is a close relationship between CMIs and lobar CMBs. We also found that the presence of CMIs was independently associated with the presence of cSS in the probable-CAA group, which was in line with the findings of a recent study [19]. In addition, we showed a spatial association between CMIs and cSS in the probable-CAA group. These findings may suggest that patients with CMIs have more severe CAA [4]. Histopathological studies with 7 T postmortem MRI have suggested that CMIs are more often involved the superficial cortical layer than the deep layers of the brains with advanced CAA, and are frequently associated with cSS after hemorrhagic transformation [37, 38]. Although there is some topographical inclination in terms of the depth in the cerebral cortices, CMIs, CMBs and cSS are distributed together with each other and are thought to be induced by CAA as a common mechanism.

We found that, compared to the probable-CAA patients with CMIs, the mix-CMB patients with CMIs showed a higher prevalence of hypertension and lacunar infarctions and severe WMH in the whole brain and basal ganglia, indicating HV as the underlying vasculopathy. In addition, when focusing on the mix-CMB group alone, the number of CMBs in the frontal lobe was associated with the presence of CMIs. These findings collectively indicate that HV is responsible mostly for CMIs in the mix-CMB patients. Our results are consistent with an observation by Pasi et al. that mix-CMBs are driven mostly by HV, although it is difficult to exclude the concomitant presence of different degree of CAA in mix-CMBs [39]. Indeed, advanced HV and CAA frequently coexist in autopsy specimens [40]; pial and cortical vessels simultaneously affected by both HV and CAA have also been observed [41]. Thus, synergistic effects of HV and CAA may lead to the development of lobar microbleeds in patients with mixed-CMBs [9, 10]. In addition, advanced CAA and HV itself promote cerebral hypoperfusion and cause a vicious cycle of Aß production and vasoconstriction of the cortical blood vessels [42].Cerebral hypoperfusion may accelerate the vascular amyloid deposition and subsequent CMI formation [31].

This study is associated with some limitations. First, the sample size was relatively small, and the statistical power was, therefore, limited. In particular, there was a small number of CMI-positive subjects, since the sensitivity of the in vivo detection of CMIs with 3 T MRI is relatively low in comparison with that with 7 T MRI [2]. Second, a recent postmortem histopathological study showed that the detection of some CMIs on standard examination is indicative of hundreds or even thousands of CMIs throughout the whole brain [43]. The size of the CMIs is variable, ranging from several hundred micrometers to 5 mm [1]. Our previous study revealed that the limit of detection was 1 mm in diameter [12]. Thus, relatively large CMIs seemed to be selectively detected in the present study. Third, we did not examine potential biomarkers for vascular amyloid deposition including amyloid-PET and the cerebrospinal fluid $A\beta_{40}$ and $A\beta_{42}$ values [44, 45]. Finally, the present results could not delineate CMIs potentially caused by microemboli, which have a distinctive pathoetiology and therapeutic strategy. They may exhibit different radiological features from CMIs due to small vessel disease [46, 47].

In conclusion, our study shows the features of CMIs in patients with multiple lobar CMBs on 3 T MRI. The CMIs in the probable-CAA group may be attributable to more severe CAA. In contrast, it is presumed that CMIs in mixed-CMBs is related to severe HV, especially when observed with more numerous lobar CMBs.

## Compliance with ethical standards

**Conflicts of interest** The authors have no conflicts of interest to disclose.

**Ethical standards** This study was approved by the ethical review board of Mie University Hospital and the requirement for written informed consent was waived because of the retrospective study design. This study was conducted in accordance with the ethical standards established in the 1964 Declaration of Helsinki and its subsequent amendments.

## References

1. Brundel M, de Bresser J, van Dillen JJ, Kappelle LJ, Biessels GJ (2012) Cerebral microinfarcts: a systematic review of neuropathological studies. J Cereb Blood Flow Metab 32:425–436
2. van Veluw SJ, Shih AY, Smith EE, Chen C, Schneider JA, Wardlaw JM, Greenberg SM, Biessels GJ (2017) Detection, risk factors, and functional consequences of cerebral microinfarcts. Lancet Neurol 16:730–740
3. Deramecourt V, Slade JY, Oakley AE, Perry RH, Ince PG, Maurage CA, Kalaria RN (2012) Staging and natural history of cerebrovascular pathology in dementia. Neurology 78:1043–1050
4. Charidimou A, Boulouis G, Gurol ME, Ayata C, Bacskai BJ, Frosch MP, Viswanathan A, Greenberg SM (2017) Emerging concepts in sporadic cerebral amyloid angiopathy. Brain 140:1829–1850
5. Linn J, Halpin A, Demaerel P, Ruhland J, Giese AD, Dichgans M, van Buchem MA, Bruckmann H, Greenberg SM (2010) Prevalence of superficial siderosis in patients with cerebral amyloid angiopathy. Neurology 74:1346–1350
6. Martinez-Ramirez S, Romero JR, Shoamanesh A, McKee AC, Van Etten E, Pontes-Neto O, Macklin EA, Ayres A, Auriel E, Himalli JJ et al (2015) Diagnostic value of lobar microbleeds in individuals without intracerebral hemorrhage. Alzheimers Dement 11:1480–1488

7. Greenberg SM, Charidimou A (2018) Diagnosis of cerebral amyloid angiopathy: evolution of the Boston criteria. Stroke 49:491–497
8. Gouw AA, Seewann A, van der Flier WM, Barkhof F, Rosemller AM, Scheltens P, Geurts JJ (2011) Heterogeneity of small vessel disease: a systematic review of MRI and histopathology correlations. J Neurol Neurosurg Psychiatry 82:126–135
9. Park JH, Seo SW, Kim C, Kim GH, Noh HJ, Kim ST, Kwak KC, Yoon U et al (2013) Pathogenesis of cerebral microbleeds: in vivo imaging of amyloid and subcortical ischemic small vessel disease in 226 individuals with cognitive impairment. Ann Neurol 73:584–593
10. Kim YJ, Kim HJ, Park JH, Kim S, Woo SY, Kwak KC, Lee JM, Jung NY et al (2016) Synergistic effects of longitudinal amyloid and vascular changes on lobar microbleeds. Neurology 87:1575–1582
11. Ii Y, Maeda M, Kida H, Matsuo K, Shindo A, Taniguchi A, Tomimoto H (2013) In vivo detection of cortical microinfarcts on ultrahigh-field MRI. J Neuroimaging 23:28–32
12. Niwa A, Ii Y, Shindo A, Matsuo K, Ishikawa H, Taniguchi A, Takase S, Maeda M, Sakuma H, Akatsu H, Hashizume Y, Tomimoto H (2017) Comparative analysis of cortical microinfarcts and microbleeds using 3.0-Tesla postmortem magnetic resonance images and histopathology. J Alzheimers Dis 59:951–959
13. Ishikawa H, Ii Y, Niwa A, Shindo A, Ito A, Matsuura K, Sasaki R, Uno K, Maeda M, Tomimoto H (2018) Comparison of premortem magnetic resonance imaging and postmortem autopsy findings of a cortical microinfarct. J Stroke Cerebrovasc Dis 27:2623–2626
14. van Dalen JW, Scuric EE, van Veluw SJ, Caan MW, Nederveen AJ, Biessels GJ, van Gool WA, Richard E (2015) Cortical microinfarcts detected in vivo on 3 Tesla MRI: clinical and radiological correlates. Stroke 46:255–257
15. van Veluw SJ, Hilal S, Kuijf HJ, Ikram MK, Xin X, Yeow TB, Venketasubramanian N, Biessels GJ, Chen C (2015) Cortical microinfarcts on 3 T MRI: clinical correlates in memory-clinic patients. Alzheimers Dement 11:1500–1509
16. Ueda Y, Satoh M, Tabei K, Kida H, Ii Y, Asahi M, Maeda M, Sakuma H, Tomimoto H (2016) Neuropsychological features of microbleeds and cortical microinfarct detected by high resolution magnetic resonance imaging. J Alzheimers Dis 53:315–325
17. Hilal S, Sikking E, Shaik MA, Chan QL, van Veluw SJ, Vrooman H, Cheng CY, Sabanayagam C et al (2016) Cortical cerebral microinfarcts on 3 T MRI: a novel marker of cerebrovascular disease. Neurology 87:1583–1590
18. van den Brink H, Zwiers A, Switzer AR, Charlton A, MaCreary CR, Goodyear BG, Frayne R, Biessels GJ, Smith EE (2018) Cortical microinfarcts on 3 T magnetic resonance imaging in cerebral amyloid angiopathy. Stroke 49:1899–1905
19. Xiong L, van Veluw SJ, Bounemia N, Charidimou A, Pasi M, Boulouis G, Reijmer YD, Giese AK et al (2018) Cerebral cortical microinfarcts on magnetic resonance imaging and their association with cognition in cerebral amyloid angiopathy. Stroke 49:2330–2336
20. van Rooden S, Goos JD, van Opstal AM, Versluis MJ, Webb AG, Blauw GJ, van der Flier WM, Scheltens P et al (2014) Increased number of microinfarcts in Alzheimer disease at 7-T MR imaging. Radiology 270:205–211
21. van Veluw SJ, Heringa SM, Kuijf HJ, Koek HL, Luijten PR, Biessels GJ (2014) Cerebral cortical microinfarcts at 7 Tesla MRI in patients with early Alzheimer's disease. J Alzheimers Dis 39:163–167
22. Fazekas F, Kleinert R, Roob G, Kleinert G, Kapeller P, Schmidt R, Hartung HP (1999) Histopathologic analysis of foci of signal loss on gradient-echo T2*-weighted MR images in patients with spontaneous intracerebral hemorrhage: evidence of microangiopathy-related microbleeds. AJNR Am J Neuroradiol 20:637–642
23. MaKhann G, Drachman D, Folstein M, Katzman R, Price D, Stadlan EM (1984) Clinical diagnosis of Alzheimer's disease: report of the NINCDS-ADRDA work group under the auspices of department of health and human services task force of Alzheimer's disease. Neurology 34:939–944
24. Bruandet A, Richard F, Bombois S, Mauraqe CA, Deramecourt V, Lebett F, Amouyel P, Pasqueir F (2009) Alzheimer's disease with cerebrovascular disease and vascular dementia: clinical features and course compared with Alzheimer's diease. J Neurol Neurosurg Psychiatry 80:133–139
25. Winblad B, Palmer K, Kivipelto M, Jelic V, Fratiglioni L, Wahlund LO, Nordberg A, Bäckman L, Albert M, Almkvist O et al (2004) Mild cognitive impairment—beyond controversies, towards a consensus: report of the International Working Group on Mild Cognitive Impairment. J Intern Med 256:240–246
26. Román GC, Tatemichi TK, Erkinjuntti T, Cummings JL, Masdeu JC, Garcia JH, Amaducci L, Orgogozo JM, Brun A, Hofman A et al (1993) Vascular dementia: diagnostic criteria for research studies. Report of the NINDS-AIREN International Workshop. Neurology 43:250–260
27. Wardlaw JM, Smith EE, Biessels GJ, Cordonnier C, Fazekas F, Frayne R, Lindlei RI, O'Brien JT, Barkhof F, Benavente OR et al (2013) Neuroimaging standards for research into small vessel disease and its contribution to ageing and neurodegeneration. Lancet Neurol 12:822–838
28. Gregoire SM, Chaudhary UJ, Brown MM, Yousry TA, Kallis C, Jäger HR, Werring DJ (2009) The microbleed anatomical rating scale (MARS): reliability of a tool to map brain microbleeds. Neurology 73:1759–1766
29. Wahlund LO, Barkhof F, Fazekas F, Bronge L, Augustin M, Sjögren M, Wallin A, Ader H, Leys D, Pantoni L et al (2001) A new rating scale for aging-related white matter changes applicable to MRI and CT. Stroke 32:1318–1322
30. Charidimou A, Linn J, Vernooij MW, Opherkr HR, Akoudad S, Baron JC, Greenberg SM, Jäger HR, Werring DJ (2015) Cortical superficial siderosis: detection and clinical significance in cerebral amyloid angiopathy and related conditions. Brain 138:2126–2139
31. Okamoto Y, Yamamoto T, Kalaria RN, Senzaki H, Maki T, Hase Y, Kitamura A, Washida K, Yamada M, Ito H, Tomimoto H, Takahashi R, Ihara M (2012) Cerebral hypoperfusion accelerates cerebral amyloid angiopathy and promotes cortical microinfarcts. Acta Neuropathol 123:381–394
32. Olichney JM, Ellis RJ, Katzman R, Sabbagh MN, Hansen L (1997) Types of cerebrovascular lesions associated with severe cerebral amyloid angiopathy in Alzheimer's disease. Ann N Y Acad Sci 826:493–497
33. Soontornniyomkij V, Lynch MD, Mermash S, Pomakian J, Badkoobehi H, Clare R, Vinters HV (2010) Cerebral microinfarcts associated with severe cerebral beta-amyloid angiopathy. Brain Pathol 20:459–467
34. Arvanitakis Z, Capuano AW, Leurgans SE, Buchman AS, Bennett DA, Schneider JA (2017) The relationship of cerebral vessel pathology to brain microinfarcts. Brain Pathol 27:77–85
35. Lauer A, van Veluw SJ, William CM, Charidimou A, Roongpiboonsopit D, Vashkevich A, Ayres A, Martinez-Ramirez S, Gurol EM, Biessels GJ et al (2016) Microbleeds on MRI are associated with microinfarcts on autopsy in cerebral amyloid angiopathy. Neurology 87:1488–1492
36. van Veluw SJ, Biessels GJ, Klijn CJ, Rozemuller AJ (2016) Heterogeneous histopathology of cortical microbleeds in cerebral amyloid angiopathy. Neurology 86:867–871
37. De Reuck J, Deramecourt V, Cordonnier C, Auger F, Durieux N, Pasquier F, Bordet R, Defebvre L, Caparros-Lefebvre D, Maurage CA, Leys D (2013) Superficial siderosis of the central nervous system: a post-mortem 7.0-Tesla magnetic resonance

imaging study with neuropathological correlates. Cerebrovasc Dis 36:412–417
38. De Reuck J, Deramecourt V, Auger F, Durieux N, Cordonnier C, Devos D, Defebvre L, Moreau C, Caparros-Lefebvre D, Bordet R, Maurage CA, Pasquier F, Leys D (2014) Post-mortem 7.0-tesla magnetic resonance study of cortical microinfarcts in neurodegenerative disease and vascular dementia with neuropathological correlates. J Neurol Sci 346:85–89
39. Pasi M, Charidimou A, Boulouis G, Auriel E, Ayres A, Schwab KM, Goldstein JN, Rosand J, Viswanasan A, Pantoni L, Greenberg SM, Gurol ME (2018) Mixed-location cerebral hemorrhage/microbleeds: underlying microangiopathy and recurrence risk. Neurology 90:e119–e126
40. Thal DR, Ghebremedhin E, Orantes M, Wiestler OD (2003) Vascular pathology in Alzheimer disease: correlation of cerebral amyloid angiopathy and arteriosclerosis/lipohyalinosis with cognitive decline. J Neuropathol Exp Neurol 62:1287–1301
41. Kövari E, Herrmann FR, Gold G, Hof PR, Charidimou A (2017) Association of cortical microinfarcts and cerebral small vessel pathology in the ageing brain. Neuropathol Appl Neurobiol 43:505–513
42. Thomas T, Miners S, Love S (2015) Post-mortem assessment of hypoperfusion of cerebral cortex in Alzheimer's disease and vascular dementia. Brain 138:1059–1069
43. Westover MB, Bianchi MT, Yang C, Schneider JA, Greenberg SM (2013) Estimating cerebral microinfarct burden from autopsy samples. Neurology 80:1365–1369
44. Charidimou A, Farid K, Baron JC (2017) Amyloid-PET in sporadic amyloid angiopathy: a diagnostic accuracy meta-analysis. Neurology 89:1490–1498
45. Renard D, Castelnovo G, Wacongne A, Le Floch A, Thouvenot E, Mas J, Gabelle A, Labauge P, Lehmann S (2012) Interest of CSF biomarker analysis in possible cerebral amyloid angiopathy cases defined by the modified Boston criteria. J Neurol 259:2429–2433
46. Landi D, Maggio P, Lupoi P, Palazzo P, Altamura C, Falato E, Altavilla R, Vollaro S, Coniglio AD, Tibuzzi F et al (2015) Cortical ischemic lesion burden measured by DIR is related to carotid artery disease severity. Cerebrovasc Dis 39:23–30
47. Takasugi J, Miwa K, Watanabe Y, Okazaki S, Todo K, Sasaki T, Sakaguchi M, Mochizuki H (2019) Cortical cerebral microinfarcts on 3 T magnetic resonance imaging in patients with carotid artery stenosis. Stroke 50:639–644